Inorganic Chemistry

Article

Cite This: Inorg. Chem. XXXX, XXX, XXX-XXX

pubs.acs.org/IC

Iron(II) Complexes of a Hemilabile SNS Amido Ligand: Synthesis, Characterization, and Reactivity

Uttam K. Das,[†] Stephanie L. Daifuku,[‡] Theresa E. Iannuzzi,[‡] Serge I. Gorelsky,[†] Ilia Korobkov,[†] Bulat Gabidullin,[†] Michael L. Neidig,*[,‡] and R. Tom Baker*[,†]

[†]Department of Chemistry and Biomolecular Sciences and Centre for Catalysis Research and Innovation, University of Ottawa, Ottawa, Ontario K1N 6N5, Canada

[‡]Department of Chemistry, University of Rochester, Rochester, New York 14627, United States

Supporting Information

ABSTRACT: We report an easily prepared bis(thioether) amine ligand, $\mathrm{S^{Me}N^{H}S^{Me}}$, along with the synthesis, characterization, and reactivity of the paramagnetic iron(II) bis(amido) complex, $[\mathrm{Fe}(\kappa^3\text{-}\mathrm{S^{Me}NS^{Me}})_2]$ (**1**). Binding of the two different thioethers to Fe generates both five- and six-membered rings with Fe−S bonds in the five-membered rings (av 2.54 Å) being significantly shorter than those in the six-membered rings (av 2.71 Å), suggesting hemilability of the latter thioethers. Consistent with this hypothesis, magnetic circular dichroism (MCD) and computational (TD-DFT) studies indicate that **1** in solution contains a five-coordinate component $[\mathrm{Fe}(\kappa^3\text{-}\mathrm{S^{Me}NS^{Me}})(\kappa^2\text{-}\mathrm{S^{Me}NS^{Me}})]$ (**2**). This ligand hemilability was demonstrated further by reactivity studies of **1** with 2,2′-bipyridine, 1,2-bis(dimethylphosphino)ethane, and 2,6-dimethylphenyl isonitrile to afford iron(II) complexes $[\mathrm{L_2Fe}(\kappa^2\text{-}\mathrm{S^{Me}NS^{Me}})_2]$ (**3**−**5**). Addition of a Brønsted acid, $\mathrm{HNTf_2}$, to **1** produces the paramagnetic, iron(II) amine−amido cation, $[\mathrm{Fe}(\kappa^3\text{-}\mathrm{S^{Me}NS^{Me}})(\kappa^3\text{-}\mathrm{S^{Me}N^{H}S^{Me}})](\mathrm{NTf_2})$ (**6**; Tf = $\mathrm{SO_2CF_3}$). Cation **6** readily undergoes amine ligand substitution by triphos, affording the 16e$^-$ complex $[\mathrm{Fe}(\kappa^2\text{-}\mathrm{S^{Me}NS^{Me}})(\kappa^3\text{-triphos})](\mathrm{NTf_2})$ (**7**; triphos = bis(2-diphenylphosphinoethyl)phenylphosphine). These complexes are characterized by elemental analysis; ^{1}H NMR, Mössbauer, IR, and UV−vis spectroscopy; and single-crystal X-ray diffraction. Preliminary results of amine−borane dehydrogenation catalysis show complex **7** to be a selective and particularly robust precatalyst.

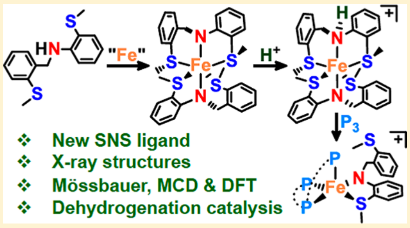

INTRODUCTION

Iron amido complexes have attracted much interest in recent years as a result of their utility in many catalytic processes including asymmetric hydrogenation,[1,2] dehydrogenation,[3−5] hydroamination,[6,7] and cross-coupling[8] reactions. For example, in asymmetric hydrogenation and transfer hydrogenation catalysis, an iron amido complex is the key intermediate in some catalytic cycles, reacting with isopropanol (in asymmetric transfer hydrogenation) or dihydrogen (in asymmetric hydrogenation) to generate an iron hydride and a secondary amine in a bifunctional mechanism.[2] Iron-mediated chemical transformations such as dinitrogen reduction,[9−12] C−H bond amination,[13,14] and olefin hydroamination[15,16] also involve iron amido species. Moreover, iron amido complexes are fundamentally important due to their diverse structural features,[17−20] unusual reactivity,[21,22] and interesting magnetic properties.[23−26] To date, numerous iron amido and imido complexes have been isolated and structurally characterized with a wide range of iron oxidation states from + I to +V.[5,17,19,20,24,27−30] In general, sterically bulky amido ligands are used to stabilize low-coordinate iron amido complexes whereas multidentate chelating amido ligands are able to stabilize coordinatively saturated compounds.

The proliferation of bifunctional catalysts has been largely due to the popularity of pincer ligands that allow for tight binding and a variety of donors including P, S, N, and C.[31−33] In our efforts to develop new bifunctional iron catalysts, we are investigating sterically svelte tridentate ligands with a mixture of hard nitrogen and soft sulfur donors capable of stabilizing a range of metal oxidation states,[34−48] and hemilabile arms that allow for substrate coordination.[49] Recently, we reported a series of mono-, di- and trinuclear iron(II) complexes containing an easily prepared tridentate thiolate ligand with thioether and imine donors, $[\mathrm{S^{Me}NS^-}]$.[50] In this work, reduction of a similar $[\mathrm{S^{Me}NS^{Me}}]$ ligand affords an amine derivative that is used to prepare new iron amido complexes containing hemilabile thioether donors. Thioether ligands usually bind weakly to first row transition metals,[38,42,48,51−54] and their hemilability has been demonstrated previously.[38,54−56] Amido groups typically form strong bonds to metals, may serve as terminal or bridging ligands, and can thus form mononuclear or multimetallic compounds. Additionally, late-metal-bound amido groups have reactive lone-pair electrons available for bifunctional substrate activation.

A variety of tridentate sulfur-containing amido ligands are known, including $[\mathrm{S^RN^-S^R}]$,[40,41,47] $[\mathrm{S^-N^-S^-}]$,[44] $[\mathrm{O^-N^-S^R}]$,[48,56] $[\mathrm{N^RN^-S^-}]$,[57] and $[\mathrm{N^-S^RN^-}]$ examples[42,58] (see corresponding secondary amines in Figure 1). It is surprising that nearly all of these sulfur-based amido ligands have been studied with

Received: July 14, 2017

DOI: 10.1021/acs.inorgchem.7b01802

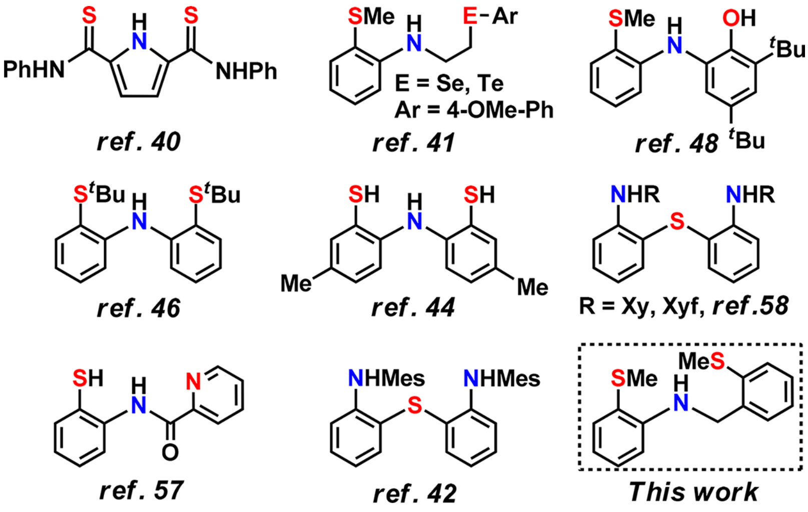

Figure 1. Sulfur-containing amines.

transition metals other than iron: Deng's group reported a few high- and low-spin iron(II) complexes employing the bulky *N,N*′-dimesityl-2,2′-diamidophenyl sulfide ligand, $[N^{-}S^{R}N^{-}]$,[42] and Mascharak and co-workers prepared and characterized an iron(III) complex bearing the *N*-2-mercaptophenyl-2′-pyridinecarboxamide ligand, $[N^{R}N^{-}S^{-}]$, which served as a structural model for nitrile hydratases.[57] Gusev et al. reported highly efficient ruthenium catalysts using a pincer-type SNS ligand, $HN(C_2H_4SEt_2)$, for bifunctional ester hydrogenation.[59] Given the importance of sulfur-based amido ligands and the well-known hemilability of thioether groups in synthetic and biological coordination chemistry as well as in bifunctional catalysis, we describe herein the synthesis and characterization of a series of iron(II) amido complexes derived from an easily prepared, unsymmetrical bis(thioether) amine ligand.

■ EXPERIMENTAL SECTION

General Considerations. Experiments were conducted under nitrogen, using Schlenk techniques or an MBraun glovebox unless otherwise stated. All solvents were deoxygenated by purging with nitrogen. Toluene, hexanes, diethyl ether, and THF were dried on columns of activated alumina using a J. C. Meyer (formerly Glass Contour) solvent purification system. [d_6]-Benzene (C_6D_6) was dried by standing over activated alumina (ca. 10 wt %) overnight, followed by filtration. Dichloromethane, [d_2]-dichloromethane (CD_2Cl_2), chloroform, and *d*-chloroform ($CDCl_3$) were dried by refluxing over calcium hydride under nitrogen. After distillation, $CDCl_3$ and dichloromethane were further dried by filtration through activated alumina (ca. 5−10 wt %). CD_2Cl_2 was vacuum-transferred before use. Ethanol (EtOH) was dried by refluxing over Mg/I_2 under nitrogen, followed by distillation. All solvents were stored over activated (heated at ca. 250 °C for >10 h under vacuum) 4 Å molecular sieves except ethanol which was stored over activated 3 Å molecular sieves. Glassware was oven-dried at 150 °C for >2 h. The following chemicals were obtained commercially, as indicated: 2-(methylthio)-benzaldehyde (Aldrich, 90%), 2-methylthioaniline (Alfa Aesar, 98%), ammonia−borane (NH_3−BH_3, Scitix, 91%), dimethylamine−borane ($(CH_3)_2NH$−BH_3, Aldrich, 97%), bipyridine (bpy, Aldrich, 98%), 2,6-dimethylphenyl isonitrile (CNxylyl, Aldrich, 96%), 1,2-bis-(dimethylphosphino)ethane (dmpe, Strem, 98%), and trimethylphosphite [$P(OMe)_3$, Strem, 97%]. ^1H, ^{19}F, and ^{31}P NMR spectra were recorded on either a 300 MHz Bruker Avance or a 300 MHz Bruker Avance II instrument at room temperature (21−25 °C). $^{13}C\{^1H\}$ NMR spectra were recorded on a 400 MHz Bruker Avance instrument. NMR spectra were referenced to the residual proton peaks associated with the deuterated solvents (for ^1H NMR, C_6D_6, δ 7.16; $CDCl_3$, δ 7.26; CD_2Cl_2, δ 5.32; and for $^{13}C\{^1H\}$ NMR, C_6D_6, δ 128.06 ppm). ^{19}F NMR spectra were referenced to internal 1,3-bis(trifluoromethyl)benzene (BTB) (Aldrich, 99%, deoxygenated by purging with nitrogen, stored over activated 4 Å molecular sieves), set to δ −63.5 ppm. ^{31}P NMR data were referenced to external H_3PO_4 (85% aqueous solution), set to δ 0.0 ppm. UV−vis spectra were recorded on an Agilent Cary 7000 universal measurement spectrophotometer, using sealable quartz cuvettes (1.0 cm path length) and dry CH_2Cl_2 or THF. IR data were collected on a Thermo Scientific Nicolet 6700 FT-IR spectrometer. Elemental analyses were performed by Elemental Analysis Service, Université de Montréal, Montréal, Québec, and by CENTC Elemental Analysis Facility, University of Rochester, Rochester, NY 14627. For electron impact (EI), solid samples were prepared by drying products under vacuum, and a Kratos Concept S1 (Hres 7000−10000) mass spectrometer was used. $[Fe\{N(SiMe_3)_2\}_2]$ was prepared by following a previously reported literature procedure.[60] The spin-only magnetic moment in solution at room temperature was obtained by the Evans method.[61]

Synthesis of the $[S^{Me}N^{H}S^{Me}]$ Ligand. *First Step: Synthesis of 2-(2-Methylthiobenzylidene)methylthioaniline.* 2-(Methylthio)-benzaldehyde (1.7 mL, 13.14 mmol) and 2-(methylthio)-aniline (1.8 mL, 14.45 mmol, 1.1 equiv) were added to a 100 mL round-bottom Schlenk flask, followed by addition of 20 mL of dry EtOH. The resulting brown solution was refluxed for 18 h under dynamic nitrogen (vented to an oil bubbler) after which no further color change was observed. The reaction mixture was cooled at −35 °C overnight after which the product precipitated as a yellow solid. Finally, the yellow product was filtered, washed with cold EtOH, and dried *in vacuo*. Yield: 3.30 g, 92% based on 2-(methylthio)-benzaldehyde. The product was used directly in the second step without further purification.

^1H NMR (300 MHz, C_6D_6 at 25 °C) δ 1.88 (s, 3H, S—Me), 2.02 (s, 3H, S—Me), 6.84−7.01 (m, 7H, Ar—H), 8.41 (d, 1H, Ar—H), 9.02 (s, 1H, N═C—H). ^{13}C NMR (101 MHz, C_6D_6) δ 14.54 (CH_3), 16.71 (CH_3), 117.90 (Ar—C), 125.03 (Ar—C), 125.38 (Ar—C), 125.84 (Ar—C), 126.64 (Ar—C), 127.97 (Ar—C), 129.61 (Ar—C), 131.49 (Ar—C), 135.05 (Ar—C), 135.29 (Ar—C), 141.12 (Ar—C), 150.14 (Ar—C), 157.62 (N═C). Figures S1 and S2 contain the ^1H and ^{13}C NMR spectra.

Second Step: Synthesis of 2-(2-Methylthiobenzyl)-methylthioaniline. 2-(2-Methylthiobenzylidene)-methylthioaniline (1.00 g, 3.66 mmol) was added to a 100 mL ampule charged with a stir bar. A 20 mL portion of THF was added to form a yellow solution, followed by 0.45 g (14.64 mmol, 4 equiv) of NH_3−BH_3. The ampule was sealed, and the resulting yellow solution was heated to 65 °C for 24 h over which time the color of the reaction mixture turned from yellow to colorless. THF was removed using vacuum, and the residue was purified using column chromatography (hexane/ethyl acetate, 4:1) to afford a white solid. Yield: 0.950 g, 94% based on 2-(2-methylthiobenzylidene)-methylthioaniline.

^{1}H NMR (300 MHz, C_6D_6 at 25 °C) δ 1.96 (s, 3H, S−Me), 2.00 (s, 3H, S−Me), 4.29 (d, 2H, ^{3}J = 5.9 Hz, −CH_2), 5.46 (t, 1H, ^{3}J = 5.9 Hz, N−H), 6.53 (dd, 1H, Ar−H), 6.59 (td, 1H, Ar−H), 6.89 (m, 1H, Ar−H), 6.99 (m, 3H, Ar−H), 7.23 (dq, 1H, Ar−H), 7.48 (dd, 1H, Ar−H). ^{13}C NMR (101 MHz, C_6D_6) δ 15.36 (CH_3), 18.13 (CH_3), 46.12 (N−C), 110.94 (Ar−C), 117.67 (Ar−C), 120.32 (Ar−C), 125.29 (Ar−C), 125.99 (Ar−C), 127.88 (Ar−C), 127.94 (Ar−C), 130.04 (Ar−C), 134.89 (Ar−C), 137.24 (Ar−C), 137.51 (Ar−C), 148.71 (Ar−C). IR (ATR, cm^{-1}): 3390 (N−H), 752 (S−Me). UV−vis (THF) λ_{max}/nm (ε/M^{-1} cm^{-1}): 291 (4300), 313 (6900). HRMS (EI, 70 eV): calcd for $C_{15}H_{17}NS_2$ m/z 275.0802 [M$^+$], found 275.0815 [M$^+$]. Anal. Calcd for $C_{15}H_{17}NS_2$: C 65.41, H 6.22, N 5.09, S 23.28. Found: C 64.89, H 6.46, N 5.04, S 23.13. Figures S3−S7 contain the ^{1}H, ^{13}C NMR, UV−vis, EI-MS, and IR spectra.

*Synthesis of [Fe(κ^3-$S^{Me}NS^{Me}$)$_2$] (**1**).* A 100 mL round-bottom Schlenk flask was charged with 2-(2-methylthiobenzyl)-methylthioaniline, [$S^{Me}N^{H}S^{Me}$] (1.00 g, 3.63 mmol), and 15 mL of hexane, yielding a white suspension. A graduated dropping funnel was charged with [Fe{N(SiMe$_3$)$_2$}$_2$] (0.684 g, 1.815 mmol, 0.5 equiv) and 10 mL of hexane giving a clear green solution. The dropping funnel was then connected to the Schlenk flask, and the green solution was added dropwise to the white suspension. Upon addition of [Fe{N(SiMe$_3$)$_2$}$_2$], the color of the reaction mixture instantly turned to yellow-green. The resulting solution was stirred for 6 h at room temperature over which period a yellow solid deposited in the bottom of the flask. After decanting the supernatant yellow-green solution, the yellow precipitate of the title complex **1** was collected by filtration using a frit followed by washing with hexane (ca. 3 × 10 mL) and diethyl ether (3 × 5 mL), and drying *in vacuo*. Yield: 1.09 g, 92% based on [Fe{N(SiMe$_3$)$_2$}$_2$]. Crystals of **1** suitable for X-ray crystallography were obtained from a concentrated toluene solution at −35 °C.

^{1}H NMR (300 MHz, C_6D_6 at 25 °C) δ −43.45 (br s, $\Delta\nu_{1/2}$ = 117 Hz), −6.35 (br s, $\Delta\nu_{1/2}$ = 251 Hz), −0.80 (br s, $\Delta\nu_{1/2}$ = 89 Hz), 6.53−6.69 (br m), 17.50 (br s, $\Delta\nu_{1/2}$ = 451 Hz), 33.35 (br s, $\Delta\nu_{1/2}$ = 249 Hz), 43.50 (br s, $\Delta\nu_{1/2}$ = 145 Hz), 66.42 (br s, $\Delta\nu_{1/2}$ = 622 Hz), 118.30 (br s, $\Delta\nu_{1/2}$ = 790 Hz). UV−vis (THF) λ_{max}/nm (ε/M^{-1} cm^{-1}): 314 (14 100), 365 (2200), 444 (1000). μ_{eff} (C_6D_6) = 4.80 μ_B. Anal. Calcd for $C_{30}H_{32}FeN_2S_4$: C 59.59, H 5.33, N 4.63, S 21.21. Found: C 58.48, H 5.38, N 4.53, S 20.43. It should be noted that the elemental analysis data for **1** are <2% low due to its high air sensitivity. Figures S8−S9 contain the ^{1}H NMR and UV−vis spectra.

*Synthesis of [Fe(κ^3-$S^{Me}NS^{Me}$)$_2$(bpy)] (**3**).* A 20 mL scintillation vial was charged with [Fe(κ^3-$S^{Me}NS^{Me}$)$_2$] (**1**) (0.200 g, 0.33 mmol), 2,2′-bipyridine (0.051 g, 0.33 mmol, 1 equiv), and THF (10 mL) affording instantly a red-brown solution. The solution was then stirred for 6 h at room temperature over which period no further color change was observed. The solution was concentrated using vacuum and left to stand at room temperature overnight to yield dark red-brown crystals (1st crop) of **3**. The red-brown filtrate was further concentrated which gave a second crop of the crystals. Finally, the dark red crystals were collected by filtration, washed with cold THF (ca. 3 × 5 mL) and diethyl ether (ca. 3 × 5 mL), and dried *in vacuo*. Combined yield was 0.201 g, 80% based on [Fe(κ^3-$S^{Me}NS^{Me}$)$_2$] (**1**).

^{1}H NMR (300 MHz, C_6D_6 at 25 °C) δ −43.20 (br s), −37.20 (br s), −13.70 (br s), −6.32 (br s), 0.25 (br s), 8.70 (br s), 17.10 (br s), 32.10 (br s), 43.73 (br s), 66.72 (br s), 118.70 (br s). UV−vis (THF) λ_{max}/nm (ε/M^{-1} cm^{-1}): 218 (45 200), 247 (39 900), 252 (37 800), 283 (15 900), 313 (8300). μ_{eff} (C_6D_6) = 4.33 μ_B. Anal. Calcd for $C_{40}H_{40}FeN_4S_4$: C 63.14, H 5.30, N 7.36. Found: C 63.31, H 5.98, N 6.60. Figure S11 shows the ^{1}H NMR spectrum.

*Synthesis of [Fe(κ^2-$S^{Me}NS^{Me}$)$_2$(CNxylyl)$_2$] (**4**).* A 20 mL scintillation vial was charged with [Fe(κ^3-$S^{Me}NS^{Me}$)$_2$] (**1**) (0.200 g, 0.33 mmol), 2,6-dimethylphenyl isonitrile, CNxylyl (0.087 g, 0.66 mmol, 2 equiv), and THF (10 mL) yielding instantly a brown solution. The solution was stirred for 6 h at room temperature over which period no further color change was observed. THF was removed under vacuum, and the resulting brown residue was washed with cold diethyl ether (ca. 3 × 5 mL) and dried *in vacuo* to give **4**. Yield: 0.229 g, 80% based on [Fe(κ^3-$S^{Me}NS^{Me}$)$_2$] (**1**).

^{1}H NMR (300 MHz, C_6D_6 at 25 °C) δ 1.72−2.43 (m, 24H, S—Me and Me—CNxylyl), 4.29 (d, 1H, —CH_2), 4.55−4.75 (m, 2H, —CH_2), 5.31−5.45 (m, 1H, —CH_2), 6.23−7.98 (m, 22H, Ar—H). ^{13}C NMR (75 MHz, C_6D_6) δ 14.38 (CH_3), 15.34 (CH_3), 15.61 (CH_3), 18.13 (CH_3), 18.60 (CH_3), 18.89 (CH_3), 46.11 (N—C), 65.92 (N—C), 109.82 (Ar—C), 110.13 (Ar—C), 110.93 (Ar—C), 115.33 (Ar—C), 117.66 (Ar—C), 120.32 (Ar—C), 123.96 (Ar—C), 124.13 (Ar—C), 125.29 (Ar—C), 124.28 (Ar—C), 125.27 (Ar—C), 125.94 (Ar—C), 126.04 (Ar—C), 126.17 (Ar—C), 127.12 (Ar—C), 127.17 (Ar—C), 127.35 (Ar—C), 127.55 (Ar—C), 127.87 (Ar—C), 127.92 (Ar—C), 127.94 (Ar—C), 128.23 (Ar—C), 130.05 (Ar—C), 132.41 (Ar—C), 134.89 (Ar—C), 135.04 (Ar—C), 135.39 (Ar—C), 135.49 (Ar—C), 136.42 (Ar—C), 136.73 (Ar—C), 137.19 (Ar—C), 137.49 (Ar—C), 139.55 (Ar—C), 140.39 (Ar—C), 148.69 (Ar—C≡N), 164.33 (Ar—C≡N). UV−vis (THF) λ_{max}/nm (ε/M^{-1} cm^{-1}): 230 (56 300), 239 (53 600), 249 (49 200), 285 (15 700), 310 (1700), 396 (3400). IR (ATR, cm^{-1}): 2054 (C≡N), 2107 (C≡N). Anal. Calcd for $C_{48}H_{50}FeN_4S_4$: C 66.49, H 5.81, N 6.46. Found: C 65.78, H 5.98, N 6.50. It is noted that due to high air sensitivity, the elemental analysis data of **4** are <2% low. Figures S12−S14 contain the ^{1}H NMR, ^{13}C NMR, and IR spectra.

*Synthesis of [Fe(κ^3-$S^{Me}NS^{Me}$)$_2$(dmpe)] (**5**).* A J-young NMR tube was charged with [Fe(κ^3-$S^{Me}NS^{Me}$)$_2$] (**1**) (0.020 g, 0.033 mmol) and 0.5 mL of CD_2Cl_2 affording a yellow solution. A 5.5 μL portion of 1,2-bis(dimethylphosphino)ethane, dmpe (0.005 g, 0.033 mmol, 1 equiv), was added to the yellow solution using a glass microsyringe. Upon addition of dmpe, no color change was observed which was confirmed by both ^{1}H and ^{31}P{^{1}H} NMR experiments at room temperature. Upon cooling to −40 °C, the color of the reaction mixture turned to brown. However, attempts to isolate and characterize the expected brown product by recrystallization at lower temperatures were unsuccessful. As a result, we could not obtain its elemental analysis. However, both ^{1}H and ^{31}P{^{1}H} NMR spectra clearly demonstrate formation of **5** at low temperature in solution.

^{1}H NMR (300 MHz, CD_2Cl_2 at −40 °C) δ 1.11 (br t, 12H, −CH_3 dmpe), 1.97 (ov s, 3H, S−Me), 1.99 (ov s, 3H, S−Me), 2.10 (s, 3H, S−Me), 2.47 (s, 3H, S−Me), 2.99 (d, 1H, ^{2}J = 18 Hz, −CH_2 dmpe), 3.58 (d, 1H, ^{2}J = 18 Hz, −CH_2 dmpe), 3.85 (d, 1H, ^{2}J = 18 Hz, −CH_2 dmpe), 4.21 (d, 1H, ^{2}J = 18 Hz, −CH_2 dmpe), 5.71 (br s, 1H, −CH_2), 6.01 (br m, 3H, −CH_2), 6.52 (br s, 1H, Ar−H), 6.69 (br s, 2H, Ar−H), 6.88 (br d, 4H, Ar−H), 7.02 (br d, 4H, Ar−H), 7.16 (br s, 2H, Ar−H), 7.34 (br d, 2H, Ar−H). ^{31}P{^{1}H} NMR (121 MHz, CD_2Cl_2 at −40 °C) δ 44.36 (d, $^{2}J_{PP}$ = 30 Hz, dmpe), 56.07 (d, $^{2}J_{PP}$ = 30 Hz, dmpe). Figures S15−S16 contain the ^{1}H and ^{31}P{^{1}H} NMR spectra.

*Synthesis of [Fe(κ^3-$S^{Me}NS^{Me}$)(κ^3-$S^{Me}N^{H}S^{Me}$)](NTf$_2$) (**6**).* A 50 mL round-bottom Schlenk flask was charged with [Fe(κ^3-$S^{Me}NS^{Me}$)$_2$] (**1**) (0.300 g, 0.496 mmol) and 10 mL of dichloromethane, yielding a yellow solution. A graduated dropping funnel (10 mL) was charged with bis(trifluoromethane)sulfonimide, HNTf$_2$ (0.139 g, 0.496 mmol, 1 equiv), and 5 mL of dichloromethane giving a clear colorless solution. The dropping funnel was then connected to the Schlenk flask, and the HNTf$_2$ solution was added dropwise to **1** affording a brick red solution. The resulting solution was stirred for 2 h at room temperature, and the solvent was removed under vacuum. The remaining red solid was then washed with diethyl ether (ca. 5 × 5 mL) and dried *in vacuo*. Yield: 0.360 g, 82% based on [Fe{N(SiMe$_3$)$_2$}$_2$]. Crystals of **7** suitable for X-ray crystallography were obtained from a concentrated dichloromethane solution at −35 °C.

^{1}H NMR (300 MHz, CD_2Cl_2 at 25 °C) δ −69.22 (br s), −42.56 (br s), −12.02 (br s), −11.05 (br s), −7.31 (br s), 0.45 (br s), 2.32 (br s), 4.30 (br s), 7.07 (br s), 8.63 (br s), 10.54 (br s), 13.68−14.58 (br m), 22.08 (br s), 25.55 (br s), 36.58 (br s), 40.96 (br s), 54.19 (br s), 81.70 (br s), 86.40 (br s), 125.70 (br s), 132.10 (br s), 152.70 (br s). ^{19}F NMR (282 MHz, $CDCl_3$) δ −66.80 (br s, $\Delta\nu_{1/2}$ = 215 Hz, Tf). UV−vis (CH_2Cl_2) λ_{max}/nm (ε/M^{-1} cm^{-1}): 312 (6800), 351 (2000). IR (ATR, cm^{-1}): 3210 (N−H). μ_{eff} ($CDCl_3$) = 5.37 μ_B Anal. Calcd for $C_{32}H_{33}F_6FeN_3O_4S_6$: C 43.39, H 3.75, N 4.74. Found: C 42.92, H 3.54, N 4.32. Figures S17−S18 contain the ^{1}H and ^{19}F NMR spectra.

DOI: 10.1021/acs.inorgchem.7b01802

*Synthesis of [Fe(κ^3-S^{Me}NS^{Me})(κ^3-triphos)] (**7**).* A 20 mL scintillation vial was charged with [Fe(κ^3-S^{Me}NS^{Me})(κ^3-S^{Me}N^{H}S^{Me})](NTf$_2$) (**6**) (0.060 g, 0.068 mmol) and triphos (0.036 g, 0.068 mmol, 1 equiv). Upon addition of 5 mL of THF, the color of the reaction mixture instantly turned to magenta. The resulting solution was stirred for 6 h at room temperature over which period no further color change was observed. THF was removed under vacuum, and the remaining dark solid was washed with benzene (ca. 4 × 5 mL) and diethyl ether (3 × 5 mL) and dried *in vacuo*. Yield: 0.051 g, 65% based on [Fe(κ^3-S^{Me}NS^{Me})(κ^3-S^{Me}N^{H}S^{Me})](NTf$_2$). Crystals of **7** suitable for X-ray crystallography were obtained from a concentrated benzene solution layered with hexane at room temperature.

^{1}H NMR (300 MHz, THF-d_8 at 25 °C) δ 2.20 (s, 3H, S−Me), 2.39 (s, 3H, S−Me), 3.11 (br m, 6H, −CH$_2$ triphos), 4.10 (br s, 2H, −CH$_2$ triphos), 5.89 (br s, 1H, −CH$_2$), 6.15 (d, 1H, −CH$_2$), 6.48−7.25 (m, 26H, Ar−H), 7.38−7.74 (m, 7H, Ar−H). ^{31}P{^{1}H} NMR (121 MHz, THF-d_8 at 25 °C) 75.60 (br s, triphos), 83.15 ppm (t, $^2J_{PP} \approx 22$ Hz, triphos); at −40 °C, 81.54 (dd, $^2J_{pp}$ = 21 Hz, 28 Hz, triphos), 74.74 (dd, $^2J_{pp}$ = 21 Hz, 28 Hz, triphos), 74.12 (t, $^2J_{pp}$ = 21 Hz, triphos). ^{19}F NMR (282 MHz, THF-d_8) δ −78.50 (br s, $\Delta\nu_{1/2}$ = 140 Hz, Tf). UV−vis (THF) λ_{max}/nm (ε/M^{-1} cm^{-1}): 251 (22 000), 311 (6600), 519 (2400). Anal. Calcd for $C_{54}H_{52}F_6FeN_2O_4P_3S_4$: C, 54.78; H, 4.43; N, 2.37. Found: C, 54.63; H, 4.42; N, 2.29. Figures S19−S21 contain the ^{1}H, ^{31}P{^{1}H}, and ^{19}F NMR spectra.

Procedure for Amine−Borane Dehydrogenation Catalysis. In a J. Young NMR tube, 3 mg of ammonia−borane (AB, 32 equiv) was mixed with 3.5 mg of **7** in THF (0.3 mL). The NMR solution was then heated at 60 °C at which time the color of the solution changed from magenta to orange. The progress of the reaction was monitored by ^{11}B, ^{11}B{^{1}H}, and ^{31}P{^{1}H} NMR spectroscopy. After 23 h, the resulting solution was filtered, and THF was removed using vacuum. The resulting solid was further characterized by ^{1}H and ^{31}P{^{1}H} NMR spectroscopy. For dehydrogenation catalysis using dimethylamine−borane (DMAB), in a J. Young NMR tube, 7.7 mg of DMAB (20 equiv) was mixed with 7.5 mg of **7** in THF (0.3 mL). The NMR solution was then heated at 60 °C in which time the color of the NMR solution changed from magenta to orange. The progress of the reaction was monitored by ^{11}B, ^{11}B{^{1}H}, and ^{31}P{^{1}H} NMR spectroscopy. After 23 h, the resulting solution was filtered, and THF was removed using vacuum. The resulting solid was then characterized by ^{1}H and ^{31}P{^{1}H} NMR spectroscopy.

■ RESULTS AND DISCUSSION

Synthesis of the [S^{Me}N^{H}S^{Me}] Ligand. We have targeted ligands that can be synthesized rapidly in one or two steps from inexpensive materials, in contrast to many of the previously reported tridentate N,S-donor ligands.[40−44,47,57,58] The tridentate ligand 2-(2-methylthiobenzyl)-methylthioaniline, [S^{Me}N^{H}S^{Me}], was prepared in two steps. Condensation of commercially available 2-(methylthio)-benzaldehyde and 2-(methylthio)-aniline in ethanol at room temperature afforded an imine ligand that was subsequently reduced to the amine in excellent yield using an excess of ammonia−borane (Scheme 1). Formation of the pure ligand was confirmed by ^{1}H, ^{13}C NMR, UV−vis, and IR spectroscopy; EI-MS; and elemental analysis.

*Synthesis and Characterization of Iron(II) Bis(amido) Complex, **1**.* The iron complex [Fe(κ^3-S^{Me}NS^{Me})$_2$] (**1**) was prepared by a transamination reaction of the [S^{Me}N^{H}S^{Me}] ligand with the low-coordinate bis(trimethylsilyl)amido iron complex, [Fe{N(SiMe$_3$)$_2$}$_2$] (Scheme 2). Slow addition of solid [Fe{N(SiMe$_3$)$_2$}$_2$] to a hexane suspension containing 2 equiv of the [S^{Me}N^{H}S^{Me}] ligand at room temperature afforded **1** as a yellow solid in 92% yield. The ^{1}H NMR spectrum of **1** shows broadened and shifted resonances ranging from 118.1 to −43.4 ppm, consistent with a paramagnetic iron center. The spectrum exhibits one set of resonances for the unsymmetrical [S^{Me}NS^{Me}] amido ligand resulting from a dynamic exchange process in solution (*vide infra*). Room temperature magnetic measurement in solution (Evans' method)[61] gave an effective magnetic moment, μ_{eff}, of 4.80 μ_B consistent with an S = 2 ground state.

The molecular structure of **1** was determined by single-crystal X-ray diffraction (Figure 2). Crystals of **1** were grown from a saturated toluene solution at −35 °C. The structure contains two [κ^3-S^{Me}NS^{Me}] amido ligands meridionally bound to the iron center. The iron center adopts a distorted octahedral geometry with *trans*-N donors. The sum of angles about N(1) and N(2) are 356.38° and 356.45°, respectively, consistent with the near planarity of the amido ligands. The

Scheme 1. Preparation of [S^{Me}N^{H}S^{Me}] Ligand

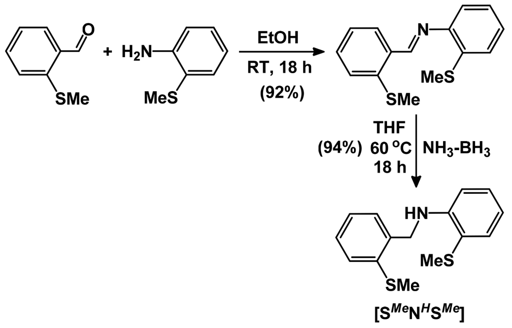

Scheme 2. Synthesis of Bis(amido) Iron(II) Complex

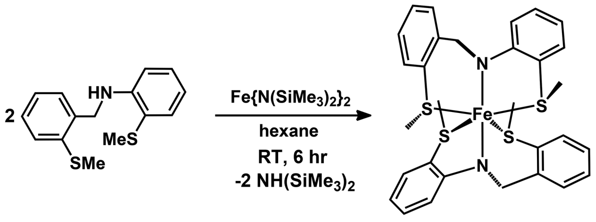

1, (92%)

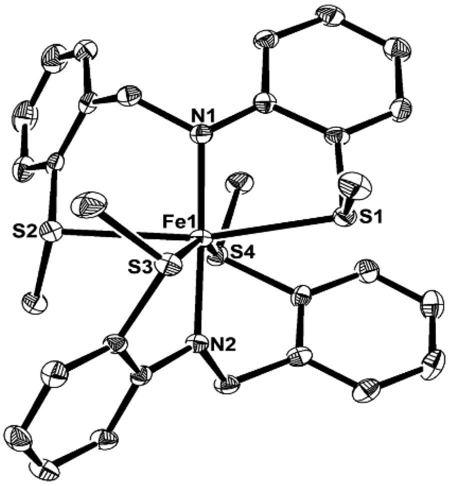

Figure 2. Molecular structure of [Fe(κ^3-S^{Me}NS^{Me})$_2$] (**1**) with 40% thermal ellipsoids. H atoms are omitted for clarity. Selected bond lengths (Å) and angles (deg): Fe(1)−S(1) 2.5389(7), Fe(1)−S(2) 2.7156(7), Fe(1)−S(3) 2.5431(7), Fe(1)−S(4) 2.7014(8), Fe(1)−N(1) 2.015(2), Fe(1)−N(2) 2.031(2), S(1)−Fe(1)−S(2) 166.63(2), S(3)−Fe(1)−S(4) 160.67(3), N(1)−Fe(1)−N(2) 177.60(8), N(1)−Fe(1)−S(1) 80.72(6), N(1)−Fe(1)−S(2) 86.80(6), N(2)−Fe(1)−S(3) 78.48(6), N(2)−Fe(1)−S(4) 95.63(6).

Fe−S distances in **1** (av Fe- S = 2.62 Å) are longer than those observed previously in high-spin iron(II) complexes with thioether ligation.[42,46,62,63] More importantly, the Fe−S distances of the six-membered metallacycle rings are significantly longer than those of the five-membered rings [e.g., 2.7156(7) and 2.7014(8) Å for Fe(1)−S(2) and Fe(1)−S(4) versus 2.5389(7) and 2.5431(7) Å for Fe(1)−S(1) and Fe(1)−S(3)]. In spite of their *trans* arrangement, the Fe−N_{amido} bond lengths (av 2.02 Å) are comparable to those found in related iron(II) amido complexes.[17−19,42] The S(1)−Fe(1)−S(2) and S(3)−Fe(1)−S(4) angles of 166.63(2)° and 160.67(3)° show significant deviation from 180° for an ideal octahedral geometry.

In order to further evaluate the electronic structure of complex **1**, Mössbauer spectroscopic and electrochemical studies were performed. Upon exposure to air, the yellow color of **1** turns initially to purple and finally to brown. The electrochemical study of **1** reveals an irreversible oxidation at 0.59 V versus ferrocene in dichloromethane solution (Figure S10). The 80 K Mössbauer spectrum of solid **1** exhibits a single quadrupole doublet with observed parameters of δ = 0.87 mm/s and ΔE_Q = 0.95 mm/s, where the isomer shift is consistent with a high-spin iron(II) species (Figure 3).[64−66]

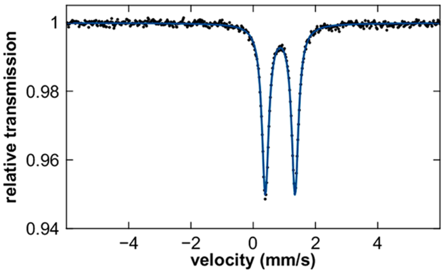

Figure 3. 80 K Mössbauer spectrum of [Fe(κ^3-$S^{Me}NS^{Me}$)$_2$] (**1**).

In order to probe the potential hemilability of the six-membered ring thioether donors, DFT optimizations of four-, five-, and six-coordinate structures of **1** were performed at the PBE/TZVP level of theory with Grimme's dispersion corrections (GD3) in the gas phase. The Gibbs free energies of five- and six-coordinate structures of **1** are very similar, with the five-coordinate structure being 0.8 kcal mol^{-1} higher in energy. The four-coordinate structure was found to be 2.5 kcal mol^{-1} higher in energy. The structural parameters for the six-coordinate structure of **1** obtained from DFT are similar to those from the X-ray structure [e.g., 2.74 and 2.73 Å for Fe(1)−S(2) and Fe(1)−S(4), 2.500 and 2.539 Å for Fe(1)−S(1) and Fe(1)−S(3)]. The calculated Mayer bond orders for Fe−S bonds are 0.25−0.27 and 0.43−0.48 for the longer and shorter bonds, respectively. Thus, the covalency of the Fe(1)−S(2) and Fe(1)−S(4) bonds is very weak. In comparison, the Fe−N bonds have bond orders of 0.61 and 0.63. As can be expected, the metal−ligand bond distances in the optimized five-coordinate structure of **1** show a small contraction relative to the six-coordinate structure, with Fe−N distances being reduced from 2.033 and 2.038 Å to 1.98 and 2.00 Å. The Fe−S distances show smaller contraction to 2.491, 2.514, and 2.74 Å. Overall, the loss of one weak covalent Fe−S bond does not cause major changes in the lengths of the remaining metal−ligand bonds. The Mayer valence index for the Fe atom in the five- and six-coordinate structures remains virtually the same (5.99 vs 6.01).

Since the solid-state structural parameters and DFT-obtained relative energies of five- and six-coordinate structures were suggestive of possible hemilability of the SNS ligand in **1**, near-infrared magnetic circular studies (NIR MCD) of **1** in frozen solution were performed. The 5 K, 7 T NIR MCD spectrum of **1** in 1/1 THF/2-Me-THF (Figure 4) contains ligand-field (LF) transitions at ∼7000 and ∼14 900 cm^{-1}.

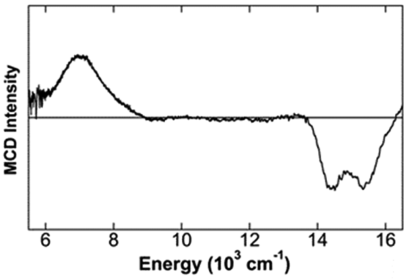

Figure 4. 5 K, 7 T NIR MCD spectrum of [Fe(κ^3-$S^{Me}NS^{Me}$)$_2$] (**1**) in 1/1 THF/2-MeTHF.

The observed transition energies are indicative of the presence of a distorted square pyramidal five-coordinate (5C) high-spin iron(II) component being present in solution,[67,68] consistent with TD-DFT calculations for 5C which predict electronic transitions at 8300 and 14200 cm^{-1}. Thus, it is clear that **1** can exist as square pyramidal complex **2**, [Fe(κ^3-$S^{Me}NS^{Me}$)(κ^2-$S^{Me}NS^{Me}$)], in solution, consistent with hemilability of the SNS ligand (Figure 5). However, it should be noted that since five-coordinate (5C) species generally exhibit much larger $\Delta\varepsilon$ values in MCD than distorted six-coordinate (6C) species, combined with the potential overlap of 6C LF transitions in the 14 000−16 000 cm^{-1} region (from TD-DFT calculations), the presence of a 6C component as well as the relative amounts of 5C versus 6C species in solution cannot be unambiguously determined.

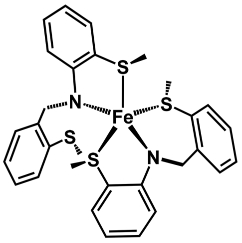

2

Figure 5. Proposed structure of [Fe(κ^3-$S^{Me}NS^{Me}$)(κ^2-$S^{Me}NS^{Me}$)] (**2**) present in solution.

To further address the amount of 5C versus 6C species that might be present in solution, frozen-solution Mössbauer studies of ^{57}Fe-enriched **1** in 1/1 THF/2-MeTHF were performed. While a reasonable fit to a single species with Mössbauer parameters nearly identical to those of **1** in the solid state was possible (Figure S28), the increased broadness in solution, slight doublet asymmetry, and reduced quality fit overall were consistent with the presence of a second, minor component at <3% of the total iron. Thus, combined with the MCD studies, the majority of **1** is 6C in solution though a minor, 5C species is also present. Even though both the MCD and TD-DFT calculations are most consistent with the square pyramidal complex **2**, we do not observe this species in the ^{1}H NMR (*vide supra*) as exchange is presumably too fast at room temperature and cooling the solution just gives complex **1**.

Reactivity Studies of Iron(II) Bis(amido) Complex, 1. Reactivity studies of complex **1** with a variety of mono- and bidentate neutral donor ligands further confirmed the hemilability of the six-membered ring thioethers. While no reaction was observed with acetonitrile, addition of 1 equiv of 2,2′-bipyridine (bpy) to **1** in THF gave an instant color change from yellow to red-brown with formation of mononuclear iron complex, [Fe(κ^2-S^{Me}NS^{Me})$_2$(bpy)] (**3**), in 80% yield (Scheme 3). The ^{1}H NMR spectrum of **3** displays broad resonances spanning a chemical shift range of 119 to −32 ppm, confirming a high-spin iron center. The room temperature magnetic measurement in solution showed an effective magnetic moment of μ_{eff} = 4.33 μ_B consistent with an S = 2 ground state. The 80 K Mössbauer spectrum of **3** is characterized by a single quadrupole doublet with observed parameters of δ = 0.96 mm/s and ΔE_Q = 2.81 mm/s, consistent with a high-spin iron(II) complex (Figure 6).[64−66]

Scheme 3. Synthesis of Paramagnetic Iron(II) Bis(SNS) Complex

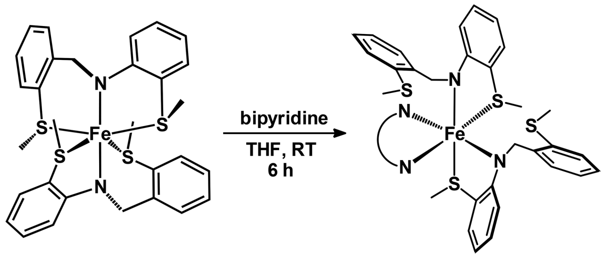

1

3, 80%

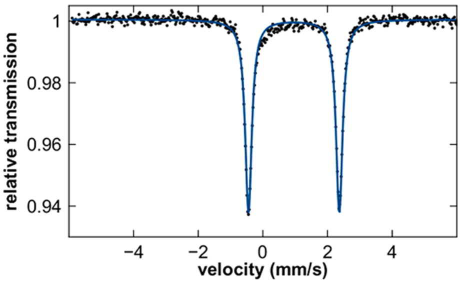

Figure 6. 80 K Mössbauer spectrum of [Fe(κ^2-S^{Me}NS^{Me})$_2$(bpy)] (**3**).

Crystals of **3** suitable for X-ray diffraction were grown from a saturated THF solution at room temperature. The structure contains two [κ^2-S^{Me}NS^{Me}] amido ligands and a κ^2-bipyridine ligand (Figure 7) in a distorted octahedral geometry about the iron. The Fe−S distances of the five-membered metalacycle rings are longer than those observed in **1** [e.g., 2.6146(4) Å for Fe(1)−S(1) and 2.6158(5) Å for Fe(1)−S(3) in **3** versus 2.5389(7) Å for Fe(1)−S(1) and 2.5431(7) Å for Fe(1)−S(3) in **1**] as well as in previously reported high-spin Fe(II) complexes with thioether ligation.[42,46,63] In contrast to **1**, the amido nitrogens in **3** are in a *cis* arrangement and the two Fe−N$_{amido}$ distances (Fe(1)−N(1) = 2.0678(13) and Fe(1)−N(2) = 2.0597(13) Å) are also slightly longer than those observed in **1** and other related iron(II) amido complexes.[17,19,42,69] The Fe−N$_{bpy}$ distances (2.2534(1) and 2.203(1) Å), on the other hand, are comparable to those previously reported for other high-spin iron(II) bipyridine complexes.[70−72] The N(2)−Fe(1)−N(3) and S(1)−Fe(1)−N(4) angles of 156.58(5)° and 159.88(4)°, respectively, deviate significantly from the ideal octahedral geometry similar to that observed in **1**. The sums of the angles about N(1) and N(2) of the amido ligands are 359.85° and 353.68°, respectively.

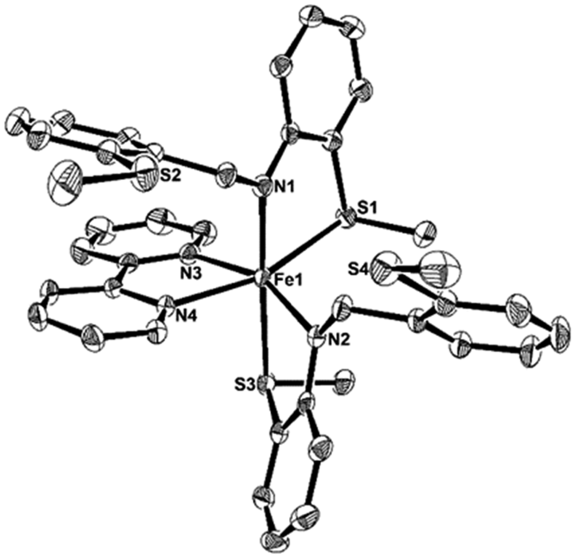

Figure 7. Molecular structure of [Fe(κ^2-S^{Me}NS^{Me})$_2$(bpy)] (**3**) with 40% thermal ellipsoids. H atoms are omitted for clarity. Selected bond lengths (Å) and angles (deg): Fe(1)−S(1) 2.6146(4), Fe(1)−S(3) 2.6158(5), Fe(1)−N(1) 2.0678(13), Fe(1)−N(2) 2.0597(13), Fe(1)−N(3) 2.2539(13), Fe(1)−N(4) 2.2030(13), N(1)−Fe(1)−S(3) 175.95(4), N(2)−Fe(1)−N(3) 156.58(5), N(4)−Fe(1)−S(1) 159.88(4), N(2)−Fe(1)−S(1) 105.08(4), N(2)−Fe(1)−N(1) 104.27(5), S(1)−Fe(1)−S(3) 97.154(14), N(2)−Fe(1)−N(4) 94.95(5), N(3)−Fe(1)−S(1) 88.95(4).

Next we examined the reactivity of **1** toward CNxylyl (2,6-dimethylphenyl isonitrile) and a chelating phosphine (i.e., 1,2-bis(dimethylphosphino)ethane, dmpe). Addition of 2 equiv of CNxylyl to a THF solution of **1** resulted in an immediate color change from yellow to brown. Removal of solvent *in vacuo* yielded a mononuclear complex, [Fe(κ^2-S^{Me}NS^{Me})$_2$(CNxylyl)$_2$] (**4**), in 80% yield (Scheme 4). The ^{1}H NMR spectrum of **4** only has resonances in the diamagnetic region, consistent with the formation of a low-spin iron(II) complex. Furthermore, the IR spectrum of **4** in the solid state shows two strong, sharp signals at 2054 and 2104 cm^{-1} which are assigned to the C−N stretching vibrations from the two *cis*-disposed isonitrile

Scheme 4. Synthesis of Diamagnetic Iron(II) Bis(SNS) Complexes

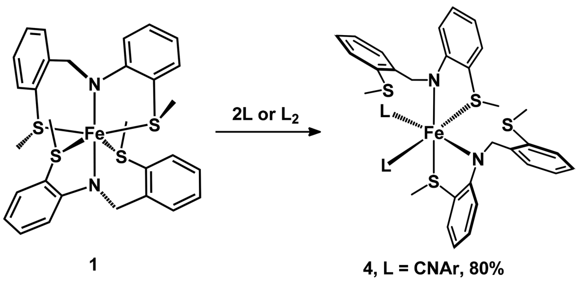

1

4, L = CNAr, 80%
5, L$_2$ = dmpe

ligands. The 80 K Mössbauer spectrum of **4** exhibits a single doublet with observed parameters of δ = 0.14 mm/s and ΔE_Q = 0.67 mm/s consistent with a low-spin, six-coordinate iron(II) complex (Figure 8).[64,73−75]

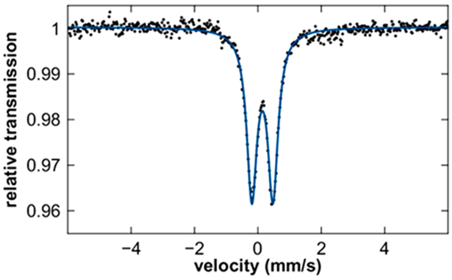

Figure 8. 80 K Mössbauer spectrum of $[\mathrm{Fe}(\kappa^2\text{-}\mathrm{S}^{Me}\mathrm{NS}^{Me})_2(\mathrm{CNxylyl})_2]$ (**4**).

However, addition of 1 equiv of dmpe to a THF solution of **1** resulted in no color change at room temperature. The ^{1}H NMR spectrum exhibited paramagnetically shifted resonances of the starting material and ^{31}P{^{1}H} NMR spectrum showed resonances of free dmpe. Upon cooling to −40 °C, the color of the reaction mixture changed from yellow to red-brown. The ^{1}H NMR spectrum of **5** at −40 °C showed resonances in the diamagnetic region, and the ^{31}P{^{1}H} NMR spectrum displayed two doublets at 56.1 and 44.4 ppm ($^2J_{PP}$ = 30 Hz), which disappeared on warming the solution to room temperature accompanied by changing color back to yellow suggesting the reversible coordination of dmpe ligand to **1**.

Formation of the Iron(II) Amine–Amido Cation, ***6.*** Deprotonated amines are usually strong bases, and therefore, one expects the basic amido donors of **1** to react with Brønsted acids. When 1 equiv of bis(trifluoromethane)sulfonimide, HNTf$_2$, was added to a solution of **1** in dichloromethane, the color changed instantly from yellow to red, yielding a cationic iron(II) complex, $[\mathrm{Fe}(\kappa^3\text{-}\mathrm{S}^{Me}\mathrm{NS}^{Me})(\kappa^3\text{-}\mathrm{S}^{Me}\mathrm{N}^{H}\mathrm{S}^{Me})](\mathrm{NTf}_2)$ (**6**), in 82% yield (Scheme 5). The ^{1}H NMR spectrum shows the paramagnetically shifted resonances of a high-spin Fe(II) complex. The ^{19}F NMR spectrum consisted of a broad singlet at −77.25 ppm assigned to the NTf$_2$ anion in the outer coordination sphere. The IR spectrum of **6** in the solid state shows a broad signal at 3488 cm^{-1} which can be attributed to an N−H stretching vibration supportive of the protonation of the amide group. Attempts to further protonate **6** were unsuccessful. The 80 K Mössbauer spectrum is also consistent with a high-spin iron(II) complex with observed parameters of δ = 0.96 mm/s and ΔE_Q = 1.92 mm/s (Figure 9).[64−66]

Scheme 5. Synthesis of Cationic Iron(II) Amine-Amido Complex

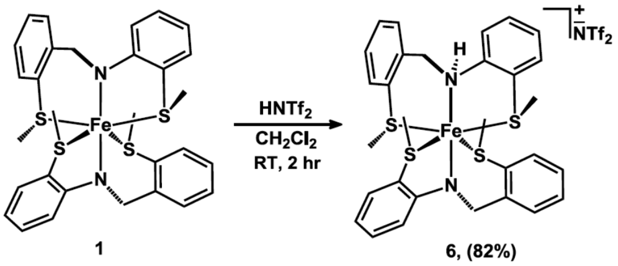

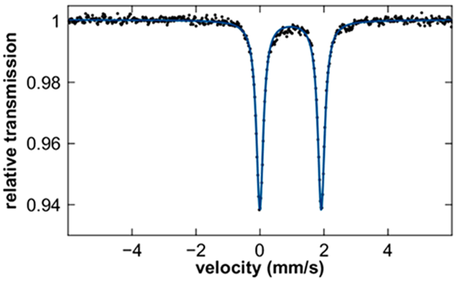

Figure 9. 80 K Mössbauer spectrum of $[\mathrm{Fe}(\kappa^3\text{-}\mathrm{S}^{Me}\mathrm{NS}^{Me})(\kappa^3\text{-}\mathrm{S}^{Me}\mathrm{N}^{H}\mathrm{S}^{Me})](\mathrm{NTf}_2)$ (**6**).

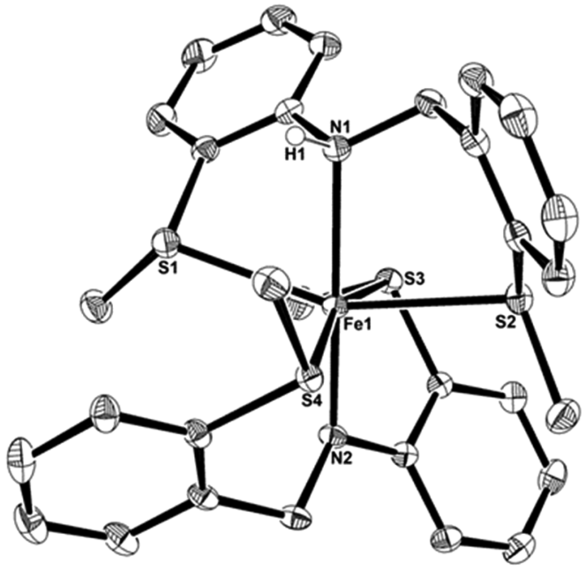

Figure 10. Molecular structure of $[\mathrm{Fe}(\kappa^3\text{-}\mathrm{S}^{Me}\mathrm{NS}^{Me})(\kappa^3\text{-}\mathrm{S}^{Me}\mathrm{N}^{H}\mathrm{S}^{Me})]$-(NTf$_2$) (**6**) with 40% thermal ellipsoids. H atom in the amine is shown, and other H atoms are omitted for clarity. Selected bond lengths (Å) and angles (deg): Fe(1)−S(1) 2.6047(6), Fe(1)−S(2) 2.6573(5), Fe(1)−S(3) 2.5200(5), Fe(1)−S(4) 2.5387(5), Fe(1)−N(1) 2.2763(15), Fe(1)−N(2) 1.9974(16), S(3)−Fe(1)−S(4) 163.403(19), N(1)−Fe(1)−S(4) 100.24(4), N(2)−Fe(1)−S(1) 108.18(5), S(3)−Fe(1)−S(1) 103.930(18), N(3)−Fe(1)−S(1) 88.95(4), S(1)−Fe(1)−S(2) 154.924(19), N(1)−Fe(1)−N(2) 173.25(6).

Crystals of **6** suitable for X-ray diffraction were grown from a saturated dichloromethane solution at −35 °C. The molecular structure consists of meridional κ^3-amido and κ^3-amine SNS ligands in a distorted octahedral geometry about iron (Figure 10). The Fe−S bond lengths of the amine ligand are longer than those of the amido ligand [e.g., 2.6047(6) Å for Fe(1)−S(1) and 2.6573(5) Å for Fe(1)−S(2) versus 2.5200(5) Å for Fe(1)−S(3) and 2.5387(5) Å for Fe(1)−S(4)]. However, both Fe−S distances of the amido [$\mathrm{S}^{Me}\mathrm{NS}^{Me}$] ligand in **6** are shorter than those found in complexes **1** and **3** (*vide supra*). The Fe−N$_{\mathrm{amine}}$ distance of 2.2763(15) Å is expectedly longer than the Fe−N$_{\mathrm{amido}}$ distance, 1.9974(16) Å. The coordination angles of the amine nitrogen in [$\mathrm{S}^{Me}\mathrm{N}^{H}\mathrm{S}^{Me}$] are consistent with the anticipated sp^3 hybridization (average of all four angles around N atom being 111.21°). The S(3)−Fe(1)−S(4) and S(1)−Fe(1)−S(2) angles of 163.40(19)° and 154.92(19)° deviate significantly from the ideal octahedral geometry. The elongated Fe−S and Fe−N$_{\mathrm{amine}}$ bonds of the [$\mathrm{S}^{Me}\mathrm{N}^{H}\mathrm{S}^{Me}$] moiety in **6** suggest that this ligand could be easily displaced by stronger donor ligands (*vide infra*).

Reactivity Studies of Iron(II) Amine–Amido Complex, ***6.*** Treatment of cation **6** with 3 equiv of $P(OMe)_3$ or CNxylyl failed to give the expected diamagnetic iron SNS amido complex. Addition of 1 equiv of bis(2-diphenylphosphinoethyl)phenyl phosphine (triphos) to a THF solution of **6** at room temperature, however, gave an instant color change from red to magenta. From this reaction, a 16e$^-$ diamagnetic iron amido complex, $[Fe(\kappa^2\text{-}S^{Me}NS^{Me})(\kappa^3\text{-triphos})](NTf_2)$ (**7**), was isolated in 65% yield (Scheme 6).

Scheme 6. Synthesis of Iron(II) Amido SNS Complex

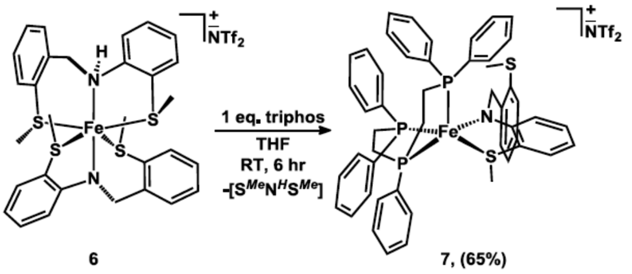

The ^{1}H NMR spectrum shows two singlets at δ 2.21 and 2.39 due to iron-bound and unbound thiomethyl groups of the SNS amido ligand. The $^{31}P\{^1H\}$ NMR spectrum shows a broad singlet and triplet at δ 77.5 and 85.0 (integration ratio: 2:1), respectively, with $^2J_{pp} \approx 22$ Hz. On cooling to −40 °C, the spectrum shows three different signals: two doublet of doublets at 81.5 and 74.7 ppm ($^2J_{pp}$ = 21 Hz, 28 Hz) and a parent triplet at 74.1 ppm ($^2J_{pp}$ = 21 Hz). It should be noted that the spectrum also contains resonances due to free triphos (10%). The 80 K Mössbauer spectrum of **7** shows a single doublet with parameters of $\delta = 0.22$ mm/s and $\Delta E_Q = 1.77$ mm/s consistent with a low-spin, five-coordinate iron(II) complex (Table 1 and Figure S29).[64,73−75]

Table 1. Experimentally Determined 80 K ^{57}Fe Mössbauer Parameters[a] for Fe(II) Complexes 1−7

Fe(II) complexes	δ (mm/s)	ΔE_Q (mm/s)	γ (mm/s)
$[Fe(\kappa^3\text{-}S^{Me}NS^{Me})_2]$ (**1**)	0.87	0.95	0.27
$[Fe(\kappa^2\text{-}S^{Me}NS^{Me})_2(bpy)]$ (**3**)	0.96	2.81	0.25
$[Fe(\kappa^2\text{-}S^{Me}NS^{Me})_2(CNxylyl)_2]$ (**4**)	0.14	0.67	0.39
$[Fe(\kappa^3\text{-}S^{Me}NS^{Me})(\kappa^3\text{-}S^{Me}N^HS^{Me})](NTf_2)$ (**6**)	0.96	1.92	0.26
$[Fe(\kappa^2\text{-}S^{Me}NS^{Me})(\kappa^3\text{-triphos})](NTf_2)$ (**7**)	0.22	1.77	0.30

[a] The error bars for the fit analyses were δ ± 0.02 mm/s and ΔE_Q ± 3%.

The molecular structure of the cation **7** was determined by X-ray diffraction (Figure 11). Crystals of **7** were grown from a saturated benzene solution layered with hexane at room temperature. The molecular structure contains a κ^3-SNS amido and a κ^3-triphos ligand in a distorted square pyramidal geometry about iron. Both Fe−N [1.921(4) Å] and Fe−S bond lengths [Fe(1)−S(1) 2.2506(18) Å] to the amido ligand are significantly shorter than those found in complexes **1**, **3**, and **6** (*vide supra*). The Fe−N distance of 1.921(4) Å is also shorter than those in complexes **1**, **3**, and **6**. The sum of three angles around N in SNS amido ligand is 357.88° (average of all three angles being 119.29°). The S(1)−Fe(1)−P(3) and N(1)−Fe(1)−P(2) angles of 158.13(7)° and 169.35(14)° deviate distinctly from the ideal square pyramidal geometry. Among three Fe−P bond distances, the apical Fe−P bond [Fe(1)−P(1) 2.1665(18) Å] is shorter than those in the basal plane [i.e., Fe(1)−P(2) 2.2205(18) and Fe(1)−P(3) 2.2395(19) Å].

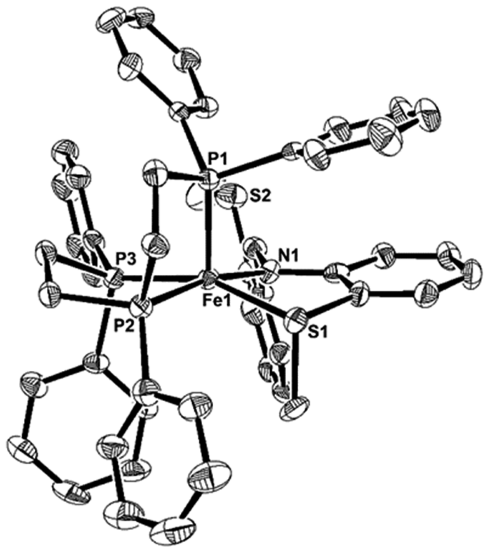

Figure 11. Molecular structure of $[Fe(\kappa^2\text{-}S^{Me}NS^{Me})(\kappa^3\text{-triphos})](NTf_2)$ (**7**) with 35% thermal ellipsoids. H atoms and NTf_2 anion are omitted for clarity. Selected bond lengths (Å) and angles (deg): Fe(1)−S(1) 2.2506(18), Fe(1)−N(1) 1.921(4), Fe(1)−P(1) 2.1665(18), Fe(1)−P(2) 2.2205(18), Fe(1)−P(3) 2.2395(19), N(1)−Fe(1)−P(2) 169.35(14), S(1)−Fe(1)−P(3) 158.13(7), S(1)−Fe(1)−P(1) 96.78(7), N(1)−Fe(1)−P(1) 103.76(15), P(3)−Fe(1)−P(1) 101.48(7), P(2)−Fe(1)−P(1) 84.74(7), S(1)−Fe(1)−P(2) 87.83(7), S(1)−Fe(1)−N(1) 84.83(14), N(1)−Fe(1)−P(3) 102.22(14), P(2)−Fe(1)−P(3) 82.00(7).

Amine−Borane Dehydrogenation Catalysis. In order to explore the relevance of the hemilability of the $[S^{Me}N^HS^{Me}]$ ligand and potential bifunctional behavior of the iron(II) amido complexes, complex **7** was assessed as a precatalyst for amine−borane dehydrogenation catalysis. At 60 °C, gas evolution was observed when a solution of **7** in THF was mixed with ammonia−borane (AB; 32 equiv). The reaction mixture changed color from magenta to orange accompanied by formation of an off-white precipitate of polyaminoborane.[76] After 23 h of heating at 60 °C, the ^{11}B NMR spectrum (Figure S22) still shows unreacted AB confirming that the dehydrogenation is slow. Product resonances include a doublet at 30.7 ppm (borazine) and a doublet, triplet, and quartet from −5 to −25 ppm which are assigned to the aminoborane tetramer, B-(cyclotriborazanyl)amine−borane (BCTB).[4] Interestingly, the $^{31}P\{^1H\}$ NMR spectrum displays only a doublet and a triplet at 88.7 and 144.6 ppm, respectively, with $^2J_{pp} \approx 30$ Hz. These resonances are correlated (gated proton decoupled ^{31}P NMR spectrum; Figure S23) with a quartet hydride resonance at δ −24.5 ($^3J_{HP} \approx 58$ Hz) in the ^{1}H NMR spectrum (Figure S24), suggestive of bifunctional AB activation. The isolation and characterization of this iron hydride complex is currently in progress to check for formation of the N−H bond.

In contrast, complex **7** shows improved catalytic activity with *N,N*-dimethylamine−borane (DMAB; 20 equiv in THF at 60 °C) affording predominantly the aminoborane cyclic dimer. While the ^{1}H NMR spectrum of the resulting orange solution again showed the quartet resonance at δ −24.1, the $^{31}P\{^1H\}$ NMR spectra showed a number of multiplet resonances, indicating less stability of the catalyst resting state with the DMAB substrate (Figure S26). Importantly, no evidence of a phosphine−borane decomposition byproduct or black solids was observed.

CONCLUSIONS

In summary, an unsymmetrical amine, 2-(2-methylthiobenzyl)-methylthioaniline, $[S^{Me}N^{H}S^{Me}]$, is readily prepared in excellent yield in two steps from commercially available starting materials. The derived pseudo-octahedral Fe(II) bis(κ^3-amido) complex, **1**, is shown by X-ray diffraction to contain two meridional tridentate ligands in the solid state with *trans*-nitrogens and two long Fe−S distances associated with six-membered metalacycle rings. Further studies using MCD and DFT calculations support the presence of a five-coordinate isomer, **2**, in solution containing one κ^2-amido ligand due to cleavage of one of the six-membered rings. Reactivity studies of **1** with a variety of donor ligands such as 2,2′-bipyridine, CNxylyl, and dmpe produced a series of high- and low-spin iron(II) bis(κ^2-amido) SNS complexes, **3**−**5**, due to cleavage of both six-membered rings. Interestingly, stable products are only formed with those ligands that can accept electron density from the iron center; the dmpe analogue is only stable at low temperatures.

Protonation of **1** with the Brønsted acid, $HNTf_2$, afforded a cationic iron(II) amine−amido complex, $[Fe(\kappa^3\text{-}S^{Me}NS^{Me})(\kappa^3\text{-}S^{Me}N^{H}S^{Me})](NTf_2)$ (**6**), which readily undergoes amine ligand displacement upon interaction with the tridentate phosphine ligand, triphos, yielding a low-spin, square pyramidal iron(II) complex, $[Fe(\kappa^2\text{-}S^{Me}NS^{Me})(\kappa^3\text{-triphos})](NTf_2)$ (**7**). Finally, complex **7** was shown to be more active as a precatalyst for dehydrogenation of dimethylamine−borane versus ammonia−borane at 60 °C, and formation of a monohydride catalyst resting state is suggestive of a bifunctional activation pathway.

Since the $[S^{Me}N^{H}S^{Me}]$ ligand is readily accessible in excellent yield and metalation is straightforward, this ligand and its analogues are well-suited for the preparation of new coordination complexes in which selective hemilability and coordination of mixed hard−soft donor groups are desirable. Given the importance of sulfur-containing amido ligands in reactivity studies and in catalysis, the $[S^{Me}NS^{Me}]$ ligand offers a new platform for developing base−metal bifunctional catalysts.

ASSOCIATED CONTENT

Supporting Information

The Supporting Information is available free of charge on the ACS Publications website at DOI: 10.1021/acs.inorgchem.7b01802.

^1H, $^{31}P\{^1H\}$, $^{13}C\{^1H\}$, and ^{19}F NMR, and IR, EI-MS, and UV−vis spectroscopic data for the ligand and iron complexes; Mössbauer and magnetic circular dichroism details and Mössbauer spectra of **1** and **7**; cyclic voltammogram of **1**; and computational details and parameters for **1** (PDF)

Accession Codes

CCDC 1562311−1562314 contain the supplementary crystallographic data for this paper. These data can be obtained free of charge via www.ccdc.cam.ac.uk/data_request/cif, or by emailing data_request@ccdc.cam.ac.uk, or by contacting The Cambridge Crystallographic Data Centre, 12 Union Road, Cambridge CB2 1EZ, UK; fax: +44 1223 336033.

AUTHOR INFORMATION

Corresponding Authors

*E-mail: neidig@chem.rochester.edu.
*E-mail: rbaker@uottawa.ca.

ORCID

R. Tom Baker: 0000-0002-1133-7149

Notes

The authors declare no competing financial interest.

ACKNOWLEDGMENTS

We thank the NSERC, the Canada Research Chairs Program, and Los Alamos National Laboratory's LDRD program for generous financial support and the University of Ottawa, Canada Foundation for Innovation, and Ontario Ministry of Economic Development and Innovation for essential infrastructure. Dr. Glenn Facey and Dr. Eric Ye are thanked for assistance with NMR experiments. M.L.N. acknowledges research support from the National Science Foundation (CHE-1454370) and from an Alfred P. Sloan Research Fellowship.

REFERENCES

(1) Zuo, W.; Tauer, S.; Prokopchuk, D. E.; Morris, R. H. Iron Catalysts Containing Amine(imine)diphosphine P-NH-N-P Ligands Catalyze both the Asymmetric Hydrogenation and Asymmetric Transfer Hydrogenation of Ketones. *Organometallics* **2014**, *33*, 5791−5801.

(2) Morris, R. H. Exploiting Metal−Ligand Bifunctional Reactions in the Design of Iron Asymmetric Hydrogenation Catalysts. *Acc. Chem. Res.* **2015**, *48*, 1494−1502.

(3) Baker, R. T.; Gordon, J. C.; Hamilton, C. W.; Henson, N. J.; Lin, P.-H.; Maguire, S.; Murugesu, M.; Scott, B. L.; Smythe, N. C. Iron Complex-Catalyzed Ammonia−Borane Dehydrogenation. A Potential Route toward B−N Containing Polymer Motifs Using Earth-Abundant Metal Catalysts. *J. Am. Chem. Soc.* **2012**, *134*, 5598−5609.

(4) Kalviri, H. A.; Gartner, F.; Ye, G.; Korobkov, I.; Baker, R. T. Probing the second dehydrogenation step in ammonia-borane dehydrocoupling: characterization and reactivity of the key intermediate, B-(cyclotriborazanyl)amine-borane. *Chem. Sci.* **2015**, *6*, 618−624.

(5) Lichtenberg, C.; Viciu, L.; Adelhardt, M.; Sutter, J.; Meyer, K.; de Bruin, B.; Grützmacher, H. Low-Valent Iron(I) Amido Olefin Complexes as Promotors for Dehydrogenation Reactions. *Angew. Chem., Int. Ed.* **2015**, *54*, 5766−5771.

(6) Greenhalgh, M. D.; Jones, A. S.; Thomas, S. P. Iron-Catalysed Hydrofunctionalisation of Alkenes and Alkynes. *ChemCatChem* **2015**, *7*, 190−222.

(7) Bernoud, E.; Oulié, P.; Guillot, R.; Mellah, M.; Hannedouche, J. Well-Defined Four-Coordinate Iron(II) Complexes For Intramolecular Hydroamination of Primary Aliphatic Alkenylamines. *Angew. Chem., Int. Ed.* **2014**, *53*, 4930−4934.

(8) Bauer, G.; Wodrich, M. D.; Scopelliti, R.; Hu, X. Iron Pincer Complexes as Catalysts and Intermediates in Alkyl−Aryl Kumada Coupling Reactions. *Organometallics* **2015**, *34*, 289−298.

(9) Crossland, J. L.; Tyler, D. R. Iron−dinitrogen coordination chemistry: Dinitrogen activation and reactivity. *Coord. Chem. Rev.* **2010**, *254*, 1883−1894.

(10) Lee, Y.; Mankad, N. P.; Peters, J. C. Triggering N_2 uptake via redox-induced expulsion of coordinated NH_3 and N_2 silylation at trigonal bipyramidal iron. *Nat. Chem.* **2010**, *2*, 558−565.

(11) Rittle, J.; Peters, J. C. An Fe-N_2 Complex That Generates Hydrazine and Ammonia via Fe=NNH_2: Demonstrating a Hybrid

Distal-to-Alternating Pathway for N_2 Reduction. *J. Am. Chem. Soc.* **2016**, *138*, 4243−4248.

(12) Rodriguez, M. M.; Bill, E.; Brennessel, W. W.; Holland, P. L. Reduction and Hydrogenation to Ammonia by a Molecular Iron-Potassium Complex. *Science* **2011**, *334*, 780−783.

(13) King, E. R.; Hennessy, E. T.; Betley, T. A. Catalytic C−H Bond Amination from High-Spin Iron Imido Complexes. *J. Am. Chem. Soc.* **2011**, *133*, 4917−4923.

(14) Che, C.-M.; Lo, V. K.-Y.; Zhou, C.-Y.; Huang, J.-S. Selective functionalisation of saturated C-H bonds with metalloporphyrin catalysts. *Chem. Soc. Rev.* **2011**, *40*, 1950−1975.

(15) Lappert, M.; Protchenko, A.; Power, P.; Seeber, A. In *Metal Amide Chemistry*; John Wiley & Sons, Ltd., 2008; pp 149−204.

(16) Beller, M.; Bolm, C. *Transition Metals for Organic Synthesis: Building Blocks and Fine Chemicals*; Wiley-VCH: Weinheim, 2004.

(17) Eckert, N. A.; Smith, J. M.; Lachicotte, R. J.; Holland, P. L. Low-Coordinate Iron(II) Amido Complexes of β-Diketiminates: Synthesis, Structure, and Reactivity. *Inorg. Chem.* **2004**, *43*, 3306−3321.

(18) Moatazedi, Z.; Katz, M. J.; Leznoff, D. B. Synthesis and characterization of a series of halide-bridged, multinuclear iron(II) and cobalt(II) diamido complexes and a dinuclear, high-spin cobalt(II) alkyl derivative. *Dalton Trans.* **2010**, *39*, 9889−9896.

(19) Wang, X.; Mo, Z.; Xiao, J.; Deng, L. Monomeric Bis(anilido)-iron(II) Complexes with N-Heterocyclic Carbene Ligation: Synthesis, Characterization, and Redox Reactivity toward Aryl Halides. *Inorg. Chem.* **2013**, *52*, 59−65.

(20) Werncke, C. G.; Bunting, P. C.; Duhayon, C.; Long, J. R.; Bontemps, S.; Sabo-Etienne, S. Two-Coordinate Iron(I) Complex $[Fe\{N(SiMe_3)_2\}_2]^-$: Synthesis, Properties, and Redox Activity. *Angew. Chem., Int. Ed.* **2015**, *54*, 245−248.

(21) Fox, D. J.; Bergman, R. G. Synthesis of a First-Row Transition Metal Parent Amido Complex and Carbon Monoxide Insertion into the Amide N−H Bond. *J. Am. Chem. Soc.* **2003**, *125*, 8984−8985.

(22) Zhao, H.; Li, X.; Zhang, S.; Sun, H. Synthesis and Characterization of Iron, Cobalt, and Nickel [PNP] Pincer Amido Complexes by N−H Activation. *Z. Anorg. Allg. Chem.* **2015**, *641*, 2435−2439.

(23) Alexander Merrill, W.; Stich, T. A.; Brynda, M.; Yeagle, G. J.; Fettinger, J. C.; Hont, R. D.; Reiff, W. M.; Schulz, C. E.; Britt, R. D.; Power, P. P. Direct Spectroscopic Observation of Large Quenching of First-Order Orbital Angular Momentum with Bending in Monomeric, Two-Coordinate Fe(II) Primary Amido Complexes and the Profound Magnetic Effects of the Absence of Jahn− and Renner−Teller Distortions in Rigorously Linear Coordination. *J. Am. Chem. Soc.* **2009**, *131*, 12693−12702.

(24) Lin, C.-Y.; Fettinger, J. C.; Grandjean, F.; Long, G. J.; Power, P. P. Synthesis, Structure, and Magnetic and Electrochemical Properties of Quasi-Linear and Linear Iron(I), Cobalt(I), and Nickel(I) Amido Complexes. *Inorg. Chem.* **2014**, *53*, 9400−9406.

(25) Eichhöfer, A.; Lan, Y.; Mereacre, V.; Bodenstein, T.; Weigend, F. Slow Magnetic Relaxation in Trigonal-Planar Mononuclear Fe(II) and Co(II) Bis(trimethylsilyl)amido Complexes-A Comparative Study. *Inorg. Chem.* **2014**, *53*, 1962−1974.

(26) Chilton, N. F.; Lei, H.; Bryan, A. M.; Grandjean, F.; Long, G. J.; Power, P. P. Ligand field influence on the electronic and magnetic properties of quasi-linear two-coordinate iron(II) complexes. *Dalton Trans.* **2015**, *44*, 11202−11211.

(27) Lucas, R. L.; Powell, D. R.; Borovik, A. S. Preparation of Iron Amido Complexes via Putative Fe(IV) Imido Intermediates. *J. Am. Chem. Soc.* **2005**, *127*, 11596−11597.

(28) Eckert, N. A.; Vaddadi, S.; Stoian, S.; Lachicotte, R. J.; Cundari, T. R.; Holland, P. L. Coordination-Number Dependence of Reactivity in an Imidoiron(III) Complex. *Angew. Chem., Int. Ed.* **2006**, *45*, 6868−6871.

(29) Ni, C.; Fettinger, J. C.; Long, G. J.; Brynda, M.; Power, P. P. Reaction of a sterically encumbered iron(I) aryl/arene with organo-azides: formation of an iron(V) bis(imide). *Chem. Commun.* **2008**, 6045−6047.

(30) Wang, L.; Hu, L.; Zhang, H.; Chen, H.; Deng, L. Three-Coordinate Iron(IV) Bisimido Complexes with Aminocarbene Ligation: Synthesis, Structure, and Reactivity. *J. Am. Chem. Soc.* **2015**, *137*, 14196−14207.

(31) Gunanathan, C.; Milstein, D. In *Bifunctional Molecular Catalysis*; Ikariya, T., Shibasaki, M., Eds.; Springer: Berlin, 2011; pp 55−84.

(32) Gunanathan, C.; Milstein, D. Bond Activation and Catalysis by Ruthenium Pincer Complexes. *Chem. Rev.* **2014**, *114*, 12024−12087.

(33) Werkmeister, S.; Junge, K.; Beller, M. Catalytic Hydrogenation of Carboxylic Acid Esters, Amides, and Nitriles with Homogeneous Catalysts. *Org. Process Res. Dev.* **2014**, *18*, 289−302.

(34) Harrop, T. C.; Mascharak, P. K. Fe(III) and Co(III) Centers with Carboxamido Nitrogen and Modified Sulfur Coordination: Lessons Learned from Nitrile Hydratase. *Acc. Chem. Res.* **2004**, *37*, 253−260.

(35) Sellmann, D.; Prakash, R.; Heinemann, F. W.; Moll, M.; Klimowicz, M. Heterolytic Cleavage of H_2 at a Sulfur-Bridged Dinuclear Ruthenium Center. *Angew. Chem., Int. Ed.* **2004**, *43*, 1877−1880.

(36) Hirotsu, M.; Santo, K.; Tsuboi, C.; Kinoshita, I. Diiron Carbonyl Complexes Bearing an N,C,S-Pincer Ligand: Reactivity toward Phosphines, Heterolytic Fe−Fe Cleavage, and Electrocatalytic Proton Reduction. *Organometallics* **2014**, *33*, 4260−4268.

(37) Imbert, C.; Hratchian, H. P.; Lanznaster, M.; Heeg, M. J.; Hryhorczuk, L. M.; McGarvey, B. R.; Schlegel, H. B.; Verani, C. N. Influence of Ligand Rigidity and Ring Substitution on the Structural and Electronic Behavior of Trivalent Iron and Gallium Complexes with Asymmetric Tridentate Ligands. *Inorg. Chem.* **2005**, *44*, 7414−7422.

(38) Klerman, Y.; Ben-Ari, E.; Diskin-Posner, Y.; Leitus, G.; Shimon, L. J. W.; Ben-David, Y.; Milstein, D. Pyridine-based SNS-iridium and -rhodium sulfide complexes, including d_8-d_8 metal-metal interactions in the solid state. *Dalton Trans.* **2008**, 3226−3234.

(39) Roy, N.; Sproules, S.; Weyhermüller, T.; Wieghardt, K. Trivalent Iron and Ruthenium Complexes with a Redox Noninnocent (2-Mercaptophenylimino)-methyl-4,6-di-tert-butylphenolate(2^-) Ligand. *Inorg. Chem.* **2009**, *48*, 3783−3791.

(40) Koizumi, T.-a.; Teratani, T.; Okamoto, K.; Yamamoto, T.; Shimoi, Y.; Kanbara, T. Nickel(II) complexes bearing a pincer ligand containing thioamide units: Comparison between SNS- and SCS-pincer ligands. *Inorg. Chim. Acta* **2010**, *363*, 2474−2480.

(41) Singh, P.; Singh, A. K. Transfer Hydrogenation of Ketones and Catalytic Oxidation of Alcohols with Half-Sandwich Complexes of Ruthenium(II) Designed Using Benzene and Tridentate (S, N, E) Type Ligands (E = S, Se, Te). *Organometallics* **2010**, *29*, 6433−6442.

(42) Xiao, J.; Deng, L. Synthesis, Structure, and Reactivity Study of Iron(II) Complexes with Bulky Bis(anilido)thioether Ligation. *Organometallics* **2012**, *31*, 428−434.

(43) Miecznikowski, J. R.; Lo, W.; Lynn, M. A.; Jain, S.; Keilich, L. C.; Kloczko, N. F.; O'Loughlin, B. E.; DiMarzio, A. P.; Foley, K. M.; Lisi, G. P.; Kwiecien, D. J.; Butrick, E. E.; Powers, E.; Al-Abbasee, R. Syntheses, characterization, density functional theory calculations, and activity of tridentate SNS zinc pincer complexes based on bis-imidazole or bis-triazole precursors. *Inorg. Chim. Acta* **2012**, *387*, 25−36.

(44) Shaffer, D. W.; Szigethy, G.; Ziller, J. W.; Heyduk, A. F. Synthesis and Characterization of a Redox-Active Bis(thiophenolato)-amide Ligand, $[SNS]^{3-}$, and the Homoleptic Tungsten Complexes, $W[SNS]_2$ and $W[ONO]_2$. *Inorg. Chem.* **2013**, *52*, 2110−2118.

(45) Widger, L. R.; Jiang, Y.; Siegler, M. A.; Kumar, D.; Latifi, R.; de Visser, S. P.; Jameson, G. N. L.; Goldberg, D. P. Synthesis and Ligand Non-Innocence of Thiolate-Ligated (N_4S) Iron(II) and Nickel(II) Bis(imino)pyridine Complexes. *Inorg. Chem.* **2013**, *52*, 10467−10480.

(46) Widger, L. R.; Jiang, Y.; McQuilken, A. C.; Yang, T.; Siegler, M. A.; Matsumura, H.; Moenne-Loccoz, P.; Kumar, D.; de Visser, S. P.; Goldberg, D. P. Thioether-ligated iron(II) and iron(III)-hydroperoxo/alkylperoxo complexes with an H-bond donor in the second coordination sphere. *Dalton Trans.* **2014**, *43*, 7522−7532.

(47) Harkins, S. B.; Peters, J. C. Amido-Bridged Cu_2N_2 Diamond Cores that Minimize Structural Reorganization and Facilitate Reversible Redox Behavior between a Cu^1Cu^1 and a Class III Delocalized $Cu^{1.5}Cu^{1.5}$ Species. *J. Am. Chem. Soc.* **2004**, *126*, 2885−2893.

(48) Ye, S.; Sarkar, B.; Lissner, F.; Schleid, T.; van Slageren, J.; Fiedler, J.; Kaim, W. Three-Spin System with a Twist: A Bis(semiquinonato)copper Complex with a Nonplanar Configuration at the Copper(II) Center. *Angew. Chem., Int. Ed.* **2005**, *44*, 2103−2106.

(49) McGuinness, D. S.; Wasserscheid, P.; Keim, W.; Morgan, D.; Dixon, J. T.; Bollmann, A.; Maumela, H.; Hess, F.; Englert, U. First Cr(III)−SNS Complexes and Their Use as Highly Efficient Catalysts for the Trimerization of Ethylene to 1-Hexene. *J. Am. Chem. Soc.* **2003**, *125*, 5272−5273.

(50) Das, U. K.; Daifuku, S. L.; Gorelsky, S. I.; Korobkov, I.; Neidig, M. L.; Le Roy, J. J.; Murugesu, M.; Baker, R. T. Mononuclear, Dinuclear, and Trinuclear Iron Complexes Featuring a New Monoanionic SNS Thiolate Ligand. *Inorg. Chem.* **2016**, *55*, 987−997.

(51) Mullen, G. E. D.; Went, M. J.; Wocadlo, S.; Powell, A. K.; Blower, P. J. Electron Transfer Induced C−S Bond Cleavage in Rhenium and Technetium Thioether Complexes: Structural and Chemical Evidence for π Back-Donation to C−S σ* Orbitals. *Angew. Chem., Int. Ed. Engl.* **1997**, *36*, 1205−1207.

(52) Ye, S.; Kaim, W.; Albrecht, M.; Lissner, F.; Schleid, T. Complexes of the imine/thioether mixed-donor ligand 8-methylthioquinoline with d^6-configurated transition metal centers: synthesis, structures and comparison with complexes of 1-methyl-2-(methylthiomethyl)-1H-benzimidazole. *Inorg. Chim. Acta* **2004**, *357*, 3325−3330.

(53) Blackwell Iii, W. C.; Bunich, D.; Concolino, T. E.; Rheingold, A. L.; Rabinovich, D. Synthesis and structure of $\{\eta^3\text{-MeSi}(CH_2SPh)_3\}$-$Cr(CO)_3$: how long can a Cr(0)−S(thioether) bond length be? *Inorg. Chem. Commun.* **2000**, *3*, 325−327.

(54) Lumsden, S. E. A.; Durgaprasad, G.; Thomas Muthiah, K. A.; Rose, M. J. Tuning coordination modes of pyridine/thioether Schiff base (NNS) ligands to mononuclear manganese carbonyls. *Dalton Trans.* **2014**, *43*, 10725−10738.

(55) Schnödt, J.; Manzur, J.; García, A.-M.; Hartenbach, I.; Su, C.-Y.; Fiedler, J.; Kaim, W. Coordination of a Hemilabile N,N,S Donor Ligand in the Redox System $[CuL_2]^{+/2+}$, L = 2-Pyridyl-N-(2′-alkylthiophenyl)methyleneimine. *Eur. J. Inorg. Chem.* **2011**, *2011*, 1436−1441.

(56) Hübner, R.; Weber, S.; Strobel, S.; Sarkar, B.; Záliš, S.; Kaim, W. Reversible Intramolecular Single-Electron Oxidative Addition Involving a Hemilabile Noninnocent Ligand. *Organometallics* **2011**, *30*, 1414−1418.

(57) Noveron, J. C.; Olmstead, M. M.; Mascharak, P. K. Effect of Carboxamido N Coordination to Iron on the Redox Potential of Low-Spin Non-Heme Iron Centers with N,S Coordination: Relevance to the Iron Site of Nitrile Hydratase. *Inorg. Chem.* **1998**, *37*, 1138−1139.

(58) Takemoto, S.; Kawamura, H.; Yamada, Y.; Okada, T.; Ono, A.; Yoshikawa, E.; Mizobe, Y.; Hidai, M. Ruthenium Complexes Containing Bis(diarylamido)/Thioether Ligands: Synthesis and Their Catalysis for the Hydrogenation of Benzonitrile. *Organometallics* **2002**, *21*, 3897−3904.

(59) Spasyuk, D.; Smith, S.; Gusev, D. G. Replacing Phosphorus with Sulfur for the Efficient Hydrogenation of Esters. *Angew. Chem., Int. Ed.* **2013**, *52*, 2538−2542.

(60) Olmstead, M. M.; Power, P. P.; Shoner, S. C. Three-coordinate iron complexes: X-ray structural characterization of the iron amide-bridged dimers $[Fe(NR_2)_2]_2$ (R = $SiMe_3$, C_6H_5) and the adduct $Fe[N(SiMe_3)_2]_2(THF)$ and determination of the association energy of the monomer $Fe\{N(SiMe_3)_2\}_2$ in solution. *Inorg. Chem.* **1991**, *30*, 2547−2551.

(61) Evans, D. F. The determination of the paramagnetic susceptibility of substances in solution by nuclear magnetic resonance. *J. Chem. Soc.* **1959**, 2003−2005.

(62) Mock, M. T.; Popescu, C. V.; Yap, G. P. A.; Dougherty, W. G.; Riordan, C. G. Monovalent Iron in a Sulfur-Rich Environment. *Inorg. Chem.* **2008**, *47*, 1889−1891.

(63) Popescu, C. V.; Mock, M. T.; Stoian, S. A.; Dougherty, W. G.; Yap, G. P. A.; Riordan, C. G. A High-Spin Organometallic Fe−S Compound: Structural and Mössbauer Spectroscopic Studies of [Phenyltris((tert-butylthio)methyl)borate]Fe(Me). *Inorg. Chem.* **2009**, *48*, 8317−8324.

(64) Gütlich, P.; Bill, E.; Trautwein, A. X. In *Mössbauer Spectroscopy and Transition Metal Chemistry: Fundamentals and Applications*; Springer-Verlag: Berlin, 2011.

(65) Weber, K.; Erdem, Ö. F.; Bill, E.; Weyhermüller, T.; Lubitz, W. Modeling the Active Site of [NiFe] Hydrogenases and the $[NiFe_u]$ Subsite of the C-Cluster of Carbon Monoxide Dehydrogenases: Low-Spin Iron(II) Versus High-Spin Iron(II). *Inorg. Chem.* **2014**, *53*, 6329−6337.

(66) Reger, D. L.; Gardinier, J. R.; Elgin, J. D.; Smith, M. D.; Hautot, D.; Long, G. J.; Grandjean, F. Structure−Function Correlations in Iron(II) Tris(pyrazolyl)borate Spin-State Crossover Complexes. *Inorg. Chem.* **2006**, *45*, 8862−8875.

(67) Neidig, M. L.; Solomon, E. I. Structure-function correlations in oxygen activating non-heme iron enzymes. *Chem. Commun.* **2005**, 5843−5863.

(68) Pavel, E. G.; Kitajima, N.; Solomon, E. I. Magnetic Circular Dichroism Spectroscopic Studies of Mononuclear Non-Heme Ferrous Model Complexes. Correlation of Excited- and Ground-State Electronic Structure with Geometry. *J. Am. Chem. Soc.* **1998**, *120*, 3949−3962.

(69) Summerscales, O. T.; Stull, J. A.; Scott, B. L.; Gordon, J. C. Syntheses and Reactivity Studies of Square-Planar Diamido−Pyridine Complexes Based on Earth-Abundant First-Row Transition Elements. *Inorg. Chem.* **2015**, *54*, 6885−6890.

(70) Zell, T.; Langer, R.; Iron, M. A.; Konstantinovski, L.; Shimon, L. J. W.; Diskin-Posner, Y.; Leitus, G.; Balaraman, E.; Ben-David, Y.; Milstein, D. Synthesis, Structures, and Dearomatization by Deprotonation of Iron Complexes Featuring Bipyridine-based PNN Pincer Ligands. *Inorg. Chem.* **2013**, *52*, 9636−9649.

(71) Real, J. A.; Muñoz, M. C.; Faus, J.; Solans, X. Spin Crossover in Novel Dihydrobis(1-pyrazolyl)borate $[H_2B(pz)_2]$-Containing Iron(II) Complexes. Synthesis, X-ray Structure, and Magnetic Properties of $[FeL\{H_2B(pz)_2\}_2]$ (L = 1,10-Phenanthroline and 2,2′-Bipyridine). *Inorg. Chem.* **1997**, *36*, 3008−3013.

(72) Irwin, M.; Jenkins, R. K.; Denning, M. S.; Krämer, T.; Grandjean, F.; Long, G. J.; Herchel, R.; McGrady, J. E.; Goicoechea, J. M. Experimental and Computational Study of the Structural and Electronic Properties of $Fe^{II}(2,2'\text{-bipyridine})(mes)_2$ and $[Fe^{II}(2,2'\text{-bipyridine})(mes)_2]^-$, a Complex Containing a 2,2′-Bipyridyl Radical Anion. *Inorg. Chem.* **2010**, *49*, 6160−6171.

(73) Liu, Y.; Xu, W.; Zhang, J.; Fuller, W.; Schulz, C. E.; Li, J. Electronic Configuration and Ligand Nature of Five-Coordinate Iron Porphyrin Carbene Complexes: An Experimental Study. *J. Am. Chem. Soc.* **2017**, *139*, 5023−5026.

(74) Ghosh, P.; Samanta, S.; Roy, S. K.; Demeshko, S.; Meyer, F.; Goswami, S. Introducing a New Azoaromatic Pincer Ligand. Isolation and Characterization of Redox Events in Its Ferrous Complexes. *Inorg. Chem.* **2014**, *53*, 4678−4686.

(75) Nasri, H.; Ellison, M. K.; Shang, M.; Schulz, C. E.; Scheidt, W. R. Variable π-Bonding in Iron(II) Porphyrinates with Nitrite, CO, and tert-Butyl Isocyanide: Characterization of $[Fe(TpivPP)(NO_2)(CO)]$. *Inorg. Chem.* **2004**, *43*, 2932−2942.

(76) Staubitz, A.; Sloan, M. E.; Robertson, A. P. M.; Friedrich, A.; Schneider, S.; Gates, P. J.; Günne, J. S. a. d.; Manners, I. Catalytic Dehydrocoupling/Dehydrogenation of N-Methylamine-Borane and Ammonia-Borane: Synthesis and Characterization of High Molecular Weight Polyaminoboranes. *J. Am. Chem. Soc.* **2010**, *132*, 13332−13345.

DOI: 10.1021/acs.inorgchem.7b01802
Inorg. Chem. XXXX, XXX, XXX−XXX